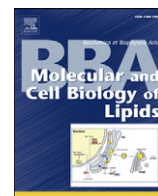Contents lists available at ScienceDirect

Biochimica et Biophysica Acta

journal homepage: www.elsevier.com/locate/bbalip

CrossMark

Lipidomic and proteomic analysis of *Caenorhabditis elegans* lipid droplets and identification of ACS-4 as a lipid droplet-associated protein

Tracy L. Vrablik [a], Vladislav A. Petyuk [b], Emily M. Larson [a], Richard D. Smith [b], Jennifer L. Watts [a,*]

[a] School of Molecular Biosciences, Washington State University, Pullman, WA 99164, USA
[b] Biological Sciences Division and Environmental Molecular Sciences Laboratory, Pacific Northwest National Laboratory, Richland, WA 99352, USA

ARTICLE INFO

ABSTRACT

Lipid droplets are cytoplasmic organelles that store neutral lipids for membrane synthesis and energy reserves. In this study, we characterized the lipid and protein composition of purified *Caenorhabditis elegans* lipid droplets. These lipid droplets are composed mainly of triacylglycerols, surrounded by a phospholipid monolayer composed primarily of phosphatidylcholine and phosphatidylethanolamine. The fatty acid composition of the triacylglycerols is rich in fatty acid species obtained from the dietary *Escherichia coli*, including cyclopropane fatty acids and cis-vaccenic acid. Unlike other organisms, *C. elegans* lipid droplets contain very little cholesterol or cholesterol esters. Comparison of the lipid droplet proteomes of wild type and high-fat *daf-2* mutant strains shows a very similar proteome in both strains, except that the most abundant protein in the *C. elegans* lipid droplet proteome, MDT-28, is relatively less abundant in lipid droplets isolated from *daf-2* mutants. Functional analysis of lipid droplet proteins identified in our proteomic studies indicated an enrichment of proteins required for growth and fat homeostasis in *C. elegans*. Finally, we confirmed the localization of one of the newly identified lipid droplet proteins, ACS-4. We found that ACS-4 localizes to the surface of lipid droplets in the *C. elegans* intestine and skin. This study bolsters *C. elegans* as a model to study the dynamics and functions of lipid droplets in a multicellular organism.

1. Introduction

A wide range of organisms store neutral lipids in cytosolic lipid droplets, which provide a reservoir of reduced hydrocarbons that can be broken down when energy is required [1]. In addition to energy storage, lipid droplets play other important functions, including sequestration of toxic proteins [2,3], protection from lipotoxicity [4], provision of precursors for membrane biosynthesis, hormones, and lipoproteins [5,6], and promotion of viral propagation [7]. In humans, too little lipid in lipid droplets is a hallmark of lipodystrophies, which are associated with diabetes and higher risk for cardiovascular and liver disease [8,9]. Too much lipid is associated with obesity and metabolic disorders such as type 2 diabetes, cardiovascular disease and ectopic lipid storage [8,10]. The highly conserved and interrelated nature of lipid metabolism across species has made model organisms pivotal for understanding the fundamental mechanisms of lipid homeostasis.

Lipid droplets are unique among organelles in that they consist of a phospholipid monolayer surrounding a core of neutral lipid. The ER is a key organelle responsible for both membrane and lipid droplet synthesis. Cytosolic lipid droplets are generally believed to arise by the accumulation of neutral lipid between the ER membrane monolayers and budding off into the cytosol (reviewed recently in [11]). Many lipid metabolic enzymes normally localized in the ER can dynamically accumulate on lipid droplets [6,12,13]. In addition to their roles in energy storage and mobilization, lipid droplets were recently implicated in signaling events, such as the regulation of cell cycle progression [14].

The free-living nematode *Caenorhabditis elegans* contains abundant lipid droplets in intestinal and hypodermal tissue. Compared to droplets in mammalian adipose tissue, which can expand to sizes of 100 μm [15], *C. elegans* lipid droplets are small, typically in the size range of 1–1.5 μm [16]. Various genetic mutations result in even smaller lipid droplets, such as stearoyl-CoA desaturase deficiency [16] or Atlastin GTPase deficiency [17], while other mutations result in larger lipid droplets, such as *daf-2* IGF receptor mutants [16], mutants in genes involved in phosphatidylcholine synthesis [18], and mutants in genes involved in peroxisomal fat oxidation [19]. Several lipid-droplet localized proteins have been characterized, including the triacylglycerol synthesis enzyme DGAT-2 [20], a putative peroxisomal beta-oxidation enzyme DHS-3 [21], the lipase ATGL-1, which accumulates on lipid droplets during fasting [22], and LID-1, a CGI-58 homolog coactivator of ATGL-1 [22]. However, the majority of proteins associated with lipid droplets have not been characterized, and differences in the lipid droplet proteomes

* Corresponding author.
E-mail address: jwatts@vetmed.wsu.edu (J.L. Watts).

among *C. elegans* mutants with altered fat accumulation have not been previously examined.

In this study, we determined the lipid and protein composition of lipid droplets isolated from wild type and the high fat *daf-2* mutant *C. elegans*. We performed RNAi knockdown of the genes encoding the most abundant lipid droplet proteins and found an enrichment of genes required for development, reproduction, and the regulation of fat homeostasis. Furthermore, we confirmed the localization of the acyl-CoA synthetase ACS-4 to the surface of lipid droplets.

2. Materials and methods

2.1. Nematode strains and growth conditions

Nematode growth media (NGM) was used to maintain *C. elegans* with OP50 *Escherichia coli* at 20 °C. The wild type strain was N2 (Bristol) and the mutant strain used in this study was CB1370 *daf-2* (*e1370*). Feeding RNAi was performed on NGM plates supplemented with 100 μg/ml ampicillin and 2 mM isopropyl-β-D-thiogalactopyranoside (IPTG) with the *E. coli* strain HT115 [23]. All HT115 strains containing RNAi constructs were sequence verified using Sanger sequencing with the primer TV10, CTGATTCTGTGGATAACCGTATAC. To grow large, synchronous populations of worms, we employed *C. elegans* liquid culture following standard protocols and using concentrated OP50 *E. coli* [24].

2.2. Isolation of C. elegans lipid droplets

C. elegans cultures from approximately 150 10 cm diameter NGM plates were collected and egg-prepped using hypochlorite bleach solution to isolate eggs from gravid hermaphrodites. Eggs were allowed to hatch overnight in M9 and a synchronized population of L1 larva was transferred to liquid culture medium and allowed to grow at 20 °C until the population reached the young adult stage. Worms were collected and washed three times to generate an approximately 8 mL dense pellet. For lipid droplet proteomics analysis, the pellet and all solutions were spiked with protease inhibitor cocktail solution (Sigma Aldrich P2714). Worms were manually chopped with razor blade tool (10–12 new razor blades taped together and sterilized with ethanol) on an ice cold glass plate until visually all the worms had been broken open. The worm pellet was then dounce homogenized 40 plunges with a tight fitting pestle. Pellet was spun at 200 ×*g* at 4 °C for 5 min and then an equal volume of 1.08 M sucrose solution was added and spun at 2000 *g* for 5 min to remove large debris. Supernatant was transferred to a 13.2 mL thinwall ultraclear centrifuge tube (Beckman-Coulter 344059) and layered with a gradient of 0.27 M sucrose, 0.135 M sucrose and Top solution buffer (25 mM Tris–HCl; 1 mM EDTA; 1 mM EGTA; protease inhibitor cocktail). Spun in SW41 rotor using a Beckman L8-70M ultracentrifuge at 35,000 rpm for 30 min at 4 °C. The top layer (white, cloudy) was transferred via a glass pipet to a siliconized microcentrifuge tube and spun at 18,000 ×*g* for 10 min and the bottom, aqueous layer was removed.

2.3. Proteomics of lipid droplets

Samples were delipidated by adding 1.5 mL of ice cold acetone and mixing well, put at −80 °C overnight and one tenth fraction removed for protein quantification. Samples were centrifuged at 7000 rpm for 1 h at 4 °C. Acetone was removed and the pellet dried down in a nitrogen stream and stored at −80 °C. Protein quantification of the aliquot was determined using the BCA quantification kit (Thermo Fisher Scientific 23225) as directed. Lipid droplet protein fractions were pooled for at least 50 μg protein per sample. The sample preparation was done in three biological replicates (3 N2 versus 3 *daf-2*) to evaluate reproducibility and statistical significance of the differential abundance values.

Given the small sample amount we decided on the trifluoroethanol based protocol [25] for preparation of the samples for the LC–MS/MS analysis. Briefly, the sample was resolubilized in 50 μl of NH_4HCO_3 (pH 7.8) using short pulses in 5510 Branson ultrasonic water bath (Branson Ultrasonics) for 3 min. After adding 50 μl of trifluoroethanol, to denature the proteins the samples were incubated at 60 °C for 2 h with gentle shaking (1000 rpm). Upon incubation the samples were diluted 5-fold with NH_4HCO_3 (pH 7.8), supplemented with trypsin (Promega) 1:25 w/w trypsin-to-protein ratio and additionally incubated for 3 h at 37 °C to digest the proteins into peptides. After the digestion, the samples were dried up using Speed-Vac and resolubilized in nanopure water. The 0.5-μg aliquots were analyzed on an LTQ Orbitrap Velos mass spectrometer that was interfaced with a 75 μm i.d. 65 cm long LC column packed with 3-μm Jupiter C18 particles (Phenomenex) as has been described before [26]. The acquired MS/MS spectra datasets were preprocessed with DeconMSn [27] and DtaRefinery [28] software followed by spectra interpretation using MSGFplus [29] software by matching against WormBase WS210 protein fasta file. The resulting peptide-to-spectrum matches were processed by MSnID Bioconductor package to ensure the maximum number of peptide identifications while not exceeding 1% of false discovery rate. After exporting the results as a spectral counting cross-tab (rows are proteins, columns are samples and values in the table are the number of MS/MS identifications of peptides belonging to a given protein) we applied Poisson-based model (using msmsTests Bioconductor package) to discover proteins differentially abundant between the lipid droplets from N2 and *daf-2* mutant strains.

2.4. Fatty acid composition and lipid analysis of isolated lipid droplets

Fatty acid composition of isolated lipid droplets and young adult nematodes was determined by gas chromatography/mass spectrometry (GC/MS) as previously described [30,31]. Separation of the TAG and phospholipid fractions used a two-solvent TLC protocol. Lipids were extracted by adding 5 ml of ice-cold chloroform:methanol (1:1) and incubating overnight at 20 °C with occasional shaking. A solution of 0.2 M H_3PO_4 and 1 M KCl was added to samples, which resulted in phase separation of the organic and aqueous phase. The organic phase was removed and dried under argon, then resuspended in chloroform. Samples were loaded in triplicate, and TLC plates were developed two thirds of the way up the plate in the first solvent system: chloroform:methanol:water:acetic acid (65:43:3:2.5), dried, and then the second solvent system hexane:diethylether:acetic acid (80:20:2) was developed to the top of the plate. Lipids were visualized under UV light after spraying the plate with 0.005% primuline, and spots corresponding to TAG and the major phospholipids were scraped, spiked with a known standard (15:0), and transesterified for GC/MS analysis to determine the fatty acid composition as well as to determine the relative levels of TAG, phosphatidylethanolamine (PE), and phosphatidylcholine (PC) fractions. At least three biological replicates were used for TLC analysis. Significance was determined by t-test calculation using GraphPad Prism 5 software.

2.5. Cholesterol assay

Cholesterol content of isolated lipid droplets was determined as described in [32]. In brief, lipids were extracted as described above and loaded on a TLC plate alongside known amounts of cholesterol and cholesterol linoleate standards. The plate was developed in a single phase hexane:ether:formic acid (80:20:2). Lipids were visualized by spraying the plate with 0.05% ferric chloride, 5% acetic and 5% sulfuric acids and heating at 160 °C for 5–10 min, when the presence of cholesterol and cholesterol esters is indicated by the appearance of red-violet colored band. A standard curve of pixel intensity was generated for the cholesterol standards using Photoshop and used to quantify the amount of cholesterol in the lipid droplet samples. To determine the levels of

cholesterol relative to TAG in lipid droplets, a second TLC plate loaded with lipid droplet samples in triplicate, separated via the same single solvent system and the amounts of TAG and PL was quantified by the above described method of GC/MS analysis.

2.6. Post-fix Nile red staining of C. elegans

RNAi of lipid droplet associated genes was performed for either the "full lifetime", from synchronized L1 animals, or "delayed start", from approximately 24 h past L1 when worms were washed and transferred to RNAi plates. All animals were allowed to grow to the young adult stage on RNAi plates and fixed Nile red staining was performed in a similar manner as described [33]. Nematodes were washed with PBS with 0.01% triton X-100 in a microcentrifuge tube. The supernatant was removed and animals were fixed with 150 μl of 40% isopropanol at room temperature for 3 min. The supernatant was removed manually, leaving 25 μl 40% isopropanol and worm pellet. To each sample 150 μl of freshly prepared Nile red staining solution (6 μl Nile red stock solution of 0.5 mg/ml in acetone per 1 ml of 40% isopropanol) was added and the tubes resealed and gently shaken in the dark for at least 2 h. Samples were allowed to settle by gravity and all but 25 μl of Nile red dye was removed and washed with 1 ml of M9 buffer. Worms were mounted on slides and imaged by fluorescent microscopy using a GFP/FITC filter. All RNAi Nile red staining experiments were performed in triplicate and blindly scored by at least two different individuals to assess alterations in fat accumulation. Images for publication were viewed with laser excitation at 488 and filtered at 495/535 nm (GFP excitation/emission) and imaged on a Leica TCS SP5 confocal microscope with a 63× oil immersion lens. Images were processed identically using Adobe Photoshop CS4.

2.7. Generation of the ACS-4::GFP strain

The strain BX265 expresses the translational fusion waEx18 (acs-4p::ACS-4::GFP). The strain was constructed using PCR to amplify the acs-4 genomic and promoter region (approximately 3 kb upstream of the ATG start site) and cloned into the pPD95.79 vector in frame to create a C terminal GFP fusion protein. The plasmid construct was microinjected into N2 worms and GFP positive worms were selected

each generation to maintain the extrachromosomal array. Worms were viewed by confocal microscopy as described in Section 2.6.

3. Results

3.1. Lipid composition of C. elegans lipid droplets

To investigate lipid droplet structure and function, we isolated lipid droplets from C. elegans and used mass spectrometry to determine their lipid and protein composition. For this analysis, we compared the lipid droplets isolated from large cultures of young adult stage wild type C. elegans with those isolated from daf-2 mutants. When grown at the restrictive temperature of 25°, daf-2 mutants arrest in the dauer larval stage. When grown at the semi-permissive temperature of 20°, daf-2 worms develop into adults that are extremely long lived and contain excess triacylglycerol stores and large lipid droplets [16,34]. Ultracentrifugation was used to isolate lipid droplets from three independent biological replicates of each genotype. Purified lipids droplets were subsequently used for proteomic analysis and lipid composition analysis.

We found that lipid droplets isolated from wild type worms contained similar lipids that made up the whole worm lipid composition, but were highly enriched in triacylglycerols (TAG). The major phospholipid (PL) components consist of phosphatidylcholine (PC) and phosphatidylethanolamine (PE) (Fig. 1A and B). While wild type whole worm lipid extracts contain a TAG/PL ratio of 1.2 (±0.2), lipid droplets contain a TAG/PL ratio of 21.3 (±2.8). The daf-2 mutants showed an even higher enrichment of TAG stores, with the whole worm TAG/PL ratio of 1.8 (±0.2) and a TAG/PL ratio in isolated daf-2 lipid droplets of 38.0 (±2.7) (Fig. 1B). Both wild type and daf-2 lipid droplets have higher PC to PE ratio than whole worm extracts, with a PC/PE ratio of 3.8 (±0.6) in wild type lipid droplets compared to a 1.3 (±0.1) ratio in whole worm extracts (Fig. 1C). These ratios were similar in daf-2 mutant worm and lipid droplet extracts (Fig. 1C). Overall, the lipid composition in C. elegans lipid droplets is similar to that described in other systems, in which lipid droplets are enriched in TAGs and the surrounding phospholipid monolayer is enriched in PC [5,35].

In addition to TAGs, the hydrophobic core of lipid droplets isolated from mammalian and yeast cells contain relatively high amounts of sterol esters [36,37]. As indicated by cholesterol staining, C. elegans membranes contain relatively low levels of sterols [38]. Thin layer
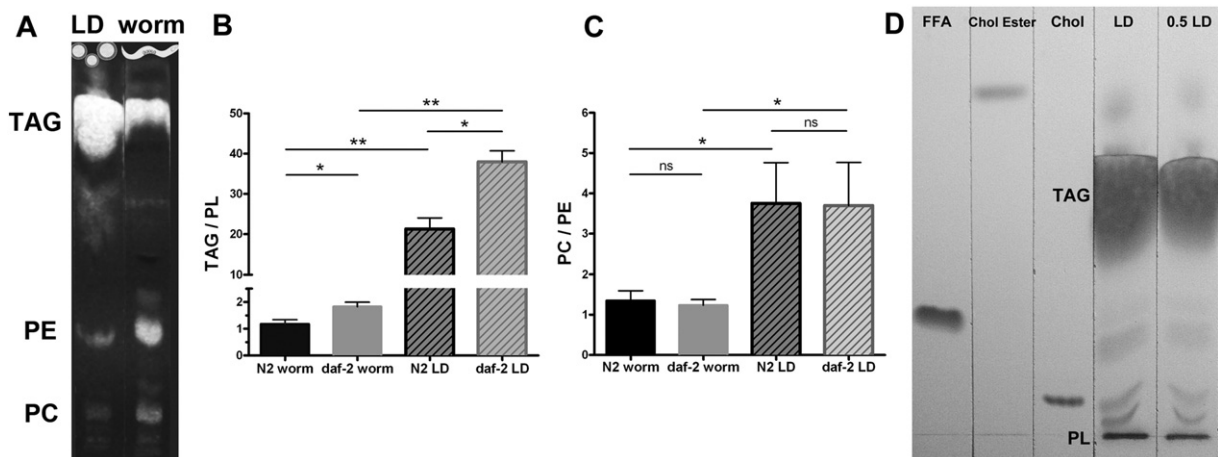

Fig. 1. Lipid analysis of isolated lipid droplets. A. Thin layer chromatography plate showing lipid fractions from isolated lipid droplets (LD, lane 1) or whole worm (lane 2), demonstrating enrichment of triacylglycerols (TAG) in the isolated lipid droplets. Other lipid classes in lipid droplets include phosphatidylethanolamine (PE) and phosphatidylcholine (PC). B. The ratio of triacylglycerols/phospholipids (TAG/PL) is increased in daf-2 whole worms and daf-2 lipid droplets compared to wild type. C. The ratio of phosphatidylcholine/phosphtidylethanolamine (PC/PE) is not different in daf-2 mutants compared to wild type. D. Very little cholesterol (Chol) or cholesterol esters (Chol ester) are present in C. elegans lipid droplets. Standards are shown in lanes 1–3 and chloroform extracts of C. elegans lipid droplets are shown in lanes 4–5. Other lipid classes include triacylglycerols (TAG), free fatty acids (FFA) and phospholipids (PL).

chromatography (TLC) separation of neutral lipids and quantification showed only trace amounts of cholesterol and cholesterol esters in lipid droplets, these compounds were present at concentrations at least 500 fold lower than TAG (Fig. 1D). This demonstrates that cholesterol and cholesterol esters are very minor components of *C. elegans* lipid droplets.

To determine the fatty acid composition of the various lipid fractions, the major phospholipid classes and TAGs were scraped from TLC plates and directly methylated to generate FAMES. MS analysis revealed the fatty acid composition of TAG in lipid droplets mirrors the composition of TAG in total worm lipid extracts (Table S1), the most abundant fatty acids were the bacterially derived cyclopropane fatty acids (17Δ and 19Δ) and cis-vaccenic acid (18:1n-7). TAG, PC, and PE constituents of lipid droplets also contained 18:DMA after derivatization, indicative of alkenyl glycerol ether lipids reported in lipid droplets of other species [36].

The fatty acid composition of *daf-2* lipid droplets contained relatively higher amounts of monounsaturated fatty acids than wild type. The TAG component of lipid droplets from *daf-2* mutants contained nearly twice as much palmitoleic acid (16:1) as wild type (6.0% in *daf-2* mutant lipid droplets compared to 3.2% in wild type lipid droplets, p = 0.005), and also contained increased cis-vaccenic acid (11.2% in *daf-2* mutants compared to 8.7% in wild type, p = 0.02). The only fatty acid showing a significantly lower relative abundance in *daf-2* mutant lipid droplets was the bacterially derived 17Δ cyclopropane fatty acid (9,10-methylene hexadecanoic acid), which made up 20.2% of the fatty acids in TAG of *daf-2* mutant lipid droplets, and 27.5% of fatty acids in the TAG component of wild type lipid droplets, p = 0.01. Thus, lipid droplets isolated from *daf-2* mutants exhibit several differences from lipid droplets isolated from wild type *C. elegans*, including an increased ratio of TAGs to PL in the *daf-2* mutants, and changes in the fatty acid composition of the TAGs.

3.2. Proteomics of wild type and daf-2 lipid droplets

Depending on the species examined, lipid droplets have been previously reported to contain from 40 to 300 different proteins [39–43]. We performed proteomic analysis on three biological replicates of N2 and *daf-2*. Our lipid droplet proteome analysis confidently identified 354 proteins belonging to various functional classes including lipid metabolism, other metabolism, transcription and translation, ribosome, trafficking and transport, cytoskeleton, chaperones, and signal transduction (Table 1, Table S2).

To estimate protein abundance we used a spectrum counting approach [44] in which the number of MS/MS spectrum identifications of the peptides belonging to a given protein were normalized (divided) by protein length (Supplemental Table 2 and Table 1). For further analysis, we focused on the top 100 most abundant proteins. The most abundant protein was MDT-28. Even though this protein shares sequence similarity to transcriptional mediator complex, it also contains an N-terminal domain similarity to pfam 03036, which is a conserved domain associated with the Perilipin family [10] (Supplemental Fig. 1). Perilipins are conserved structural components of lipid droplets that regulate lipid storage and hydrolysis [10].

The most striking difference we found between the lipid droplet proteomes of wild type and the long-lived, high fat *daf-2* mutants was in the abundance of MDT-28 protein. The *daf-2* lipid droplets, which are larger than wild type, contain relatively less MDT-28 protein, approximately 70% of wild type. This indicates that MDT-28 protein might be an important regulator of lipid droplet metabolism. Besides the difference in MDT-28 protein in wild type vs. *daf-2*, very few other proteins showed differential abundance in these strains, only 10/354 proteins (2.8%) showed significantly different abundance in *daf-2* vs. wild type *C. elegans*, with 8/10 proteins showing reduced abundance in the lipid droplets of *daf-2* mutants (Table S2).

After we started our analysis, the proteome of lipid droplets isolated from two biological replicates from wild type *C. elegans* was reported [21]. Although worms were grown using different methods for each study, and slightly different purification methods were used, the same dietary *E. coli* strain was used as food and lipid droplets were isolated from similar life stages in both studies. We found similar overlap among lipid droplet proteins from two studies, with nearly two thirds (63%) of our top 100 proteins present in Zhang et al. proteome (Table 1).

Functional analysis of lipid droplet proteins

To determine the roles of lipid droplet proteins in *C. elegans* growth and fat accumulation, we performed RNAi knockdown using the feeding method, focusing on the top 100 most abundant *C. elegans* LD proteins (Table 1). Of the 37 non-ribosomal/translation factor proteins, we obtained 21 sequence-verified RNAi constructs. Nine out of 21 showed an RNAi phenotype of arrested growth or sterility. Of the 63 ribosome/translation factor genes, we knocked down a subset of 18 of them. Of this class, all 18 resulted in arrested growth. Thus, of the set of 37 genes knocked down using RNAi, we found an enrichment of essential genes (73%). This is a much higher proportion of essential genes than have been typically identified in whole genome RNAi screens, revealing approximately 10% essential genes [45] (Table 1).

We stained the RNAi treated nematodes with post-fix Nile red to assess fat accumulation at the young adult stage. Fat accumulation depends on growth stage, so we were careful to synchronize worms and stain all strains after the L4-YA molt, but before the formation of eggs. In the 21 non-ribosomal knockdowns, we stained the 12 normal growing strains and found six of them affect fat accumulation: *acs-4*, *cey-2*, and *vit-6* RNAi resulted in increased fat accumulation, while *tkt-1*, *ant-1.1*, and *mdt-28* showed reduced fat (Fig. 2). In the arrested treatments, including the ribosomal/translation class, we waited until L3 stage to shift wild type worms to RNAi treatment and stained for fat 24 h later. Of the nine non-ribosomal strains, five affected fat accumulation. Of the 18 ribosomal/translation factor strains, four affected fat accumulation (Fig. 2). Overall, 14/37 strains, 38% showed changes in fat accumulation, much higher than the percentage of fat regulatory genes in the overall genome. For example, in a recent study 37/1600 genes (2.3%) were identified that affected lipid accumulation [46]. Thus, our functional studies demonstrate that lipid droplet associated proteins are enriched for essential proteins as well as proteins that influence fat accumulation in *C. elegans*.

3.4. Lipid droplet abnormalities in the mdt-28 knockdown germ line

In early embryos, lipid droplets and yolk particles are abundant, providing precursors for membrane synthesis during rapid cell division as well as energy for cellular processes until hatching. Fixed Nile red staining showed abnormal lipid droplets in *mdt-28*(*RNAi*) oocytes and embryos compared to the empty vector control. Individual lipid droplets are easily distinguishable in control oocytes and in the early stage embryo, however, lipid droplets in *mdt-28*(*RNAi*) oocytes and embryos clump together, giving the appearance of brighter lipid staining in the *mdt-28*(*RNAi*) germ line (Fig. 3). However, this abnormal lipid droplet appearance does not seem to affect embryonic development, as no abnormal late stage embryos were observed in the *mdt-28*(*RNAi*) worms. This observation implies that MDT-28 might be especially important in the formation or stabilization of lipid droplets in the germ line.

3.5. ACS-4 localizes to C. elegans lipid droplets

One of the lipid droplet proteins identified in this study was ACS-4, a member of the acyl-CoA synthetase family. ACS proteins catalyze the addition of coenzyme A to fatty acids, activating them for further lipid synthesis, fatty acid catabolism, and transport of fatty acids between

Table 1

Functional categories and RNAi phenotypes of the 100 most abundant lipid droplet proteins in *C. elegans*.

Gene	Rank of abundance in N2	Different in daf-2?	Growth	Fixed Nile red	Late start Nile red	Function	Zhang et al.
mdt-28	1	Lower	Normal	LF, clumps in embryos		Structure?	Yes
Metabolism							
F22F7.1	21		Normal	WT		Oxidoreductase	Yes
dhs-3	36		No RNAi			Dehydrogenase	Yes
F46H5.3	42		Normal	WT		Arginine kinase	No
Y7A5A.1	55		Normal	WT		Oxidoreductase	Yes
ahcy-1	59	Lower	Slow/sterile		HF	S-adenosylhomocysteine hydrolase	No
Y53F4B.18	63	Lower	No RNAi			FAAH homolog	Yes
acs-4	65		Normal	HF		Acetyl-CoA synthetase	Yes
alh-4	77		No RNAi			Aldehyde dehydrogenase	Yes
tkt-1	92		Normal	LF		Pentose phosphate pathway	No
Mitochondria							
ant-1.1	17		Slow/sterile		LF		Yes
vdac-1	22		Normal	WT		Mitochondrial outer membrane channel	Yes
F45H10.2	45		Slow/sterile		LF	Cytochrome b-c1 complex subunit	Yes
phb-1	83		No rnai			Mitochondrial prohibitin complex	Yes
F54A3.5	85		No RNAi			Mitochondrial inner membrane protein	Yes
atp-2	96		Arrested		WT	ATP synthase complex	Yes
Miscellaneous cytoplasmic							
rab-1	24		Arrested		WT	GTPase	Yes
hsp-1	48	Lower	Arrested		HF	Chaperone	Yes
vha-8	51		Arrested		WT	Vacuolar ATPase	No
T09A12.5	57		No RNAi			Stress-associated ER protein	Yes
sip-1	62	Higher	Normal	WT		Chaperone	Yes
pab-1	74	Lower	Slow	WT		RNA binding	No
Y38F2AR.9	75		No RNAi			Sec61 ER translocation	No
act-5	81		Arrested		LF	Cytoplasmic actin	Yes
ndk-1	86		Normal	WT		Nucleoside diphosphate kinase	No
cey-2	88	Lower	Normal	HF		RNA binding	No
Y67H2A.5	90		No RNAi			KASH domain protein	Yes
crt-1	97		No RNAi				Yes
fkb-2	99		Normal		WT	Protein folding	No
Yolk proteins							
vit-6	40		Normal	HF		Vitellogenin, yolk protein	Yes
vit-2	91		No RNAi			Vitellogenin, yolk protein	Yes
Ribosome/translation							
rpl-18	2		Arrested		WT	Large subunit ribosome	Yes
rps-13	3		Arrested		WT	Small subunit ribosome	Yes
rpl-13	4		Arrested		WT	Large subunit ribosome	Yes
rpl-4	5					Large subunit ribosome	Yes
rpl-16	6					Large subunit ribosome	No
rps-15	7		Arrested		HF	Small subunit ribosome	Yes
rpl-7	8		Very slow		WT	Large subunit ribosome	Yes
rps-8	9		Arrested		WT	Small subunit ribosome	Yes
rps-26	10		Very slow		WT	Small subunit ribosome	No
rpl-19	11		Arrested		HF	Large subunit ribosome	Yes
rpl-36	12					Large subunit ribosome	Yes
rpl-2	13		Arrested		WT	Large subunit ribosome	Yes
rpl-15	14					Large subunit ribosome	No
rpl-10	15		Arrested		WT	Large subunit ribosome	Yes
rpl-34	16					Large subunit ribosome	No
rpl-17	18					Large subunit ribosome	No
rpl-24.1	19		Arrested		WT	Large subunit ribosome	No
Y37E3.8	20					Large subunit ribosome	No
rla-1	23					Large subunit ribosome	Yes
rps-9	25		Arrested		HF	Small subunit ribosome	No
rpl-3	26		Arrested		WT	Large subunit ribosome	Yes
Y73B3A.18	27					Large subunit ribosome	No
rps-11	28					Small subunit ribosome	Yes
rpl-22	29					Large subunit ribosome	No
rpl-21	30					Large subunit ribosome	No
rpl-5	31		Arrested		WT	Large subunit ribosome	Yes
rpl-1	32					Large subunit ribosome	Yes
rps-14	33					Small subunit ribosome	No
rps-27	34					Small subunit ribosome	No
rps-1	35		Arrested		WT	Small subunit ribosome	Yes
rps-4	37					Small subunit ribosome	Yes
rps-18	38					Small subunit ribosome	No
rps-6	39					Small subunit ribosome	Yes
rps-2	41		Arrested		WT	Small subunit ribosome	Yes
rpl-32	43					Large subunit ribosome	Yes

Table 1 (*continued*)

Gene	Rank of abundance in N2	Different in daf-2?	Growth	Fixed Nile red	Late start Nile red	Function	Zhang et al.
rpl-35	44					Large subunit ribosome	Yes
rla-0	46		very slow		WT	Large subunit ribosome	Yes
rps-20	47					Small subunit ribosome	No
rpl-33	49					Large subunit ribosome	No
eef-2	50		Arrested		HF	Translation elongation factor	Yes
rpl-6	52					Large subunit ribosome	No
rps-7	53					Small subunit ribosome	Yes
rps-24	54					Small subunit ribosome	No
rps-3	56					Small subunit ribosome	Yes
rps-22	58					Small subunit ribosome	Yes
rpl-9	60					Large subunit ribosome	Yes
eef-1A.2	61					Translation elongation factor	Yes
rpl-26	64					Large subunit ribosome	No
rpl-31	66					Large subunit ribosome	Yes
eef-1B.1	67					Translation elongation factor	No
rpl-27	69					Large subunit ribosome	Yes
rpl-20	70					Large subunit ribosome	No
rps-16	71					Small subunit ribosome	Yes
rps-10	72					Small subunit ribosome	Yes
rps-19	73					Small subunit ribosome	Yes
rps-0	76					Small subunit ribosome	Yes
rpl-14	78					Large subunit ribosome	No
rps-17	80					Small subunit ribosome	Yes
eef-1G	84					Translation elongation factor	No
rps-23	87					Small subunit ribosome	No
rpl-23	93					Large subunit ribosome	Yes
rpl-25.2	94					Large subunit ribosome	No
rpl-25.1	95					Large subunit ribosome	No
Unknown function							
R06B9.5	68						No
tct-1	79						No
F44E5.1	82						Yes
ril-1	89						No
C32E8.4	98						No
K12H4.5	100						No

Abbreviations: HF, high fat; LF, low fat; WT, wild type.

subcellular compartments [47]. To determine if ACS-4 is a bonafide *C. elegans* lipid droplet protein, we created a transgenic strain expressing an extrachromosomal array consisting of *acs-4* promoter and genomic sequences fused in frame to GFP. Live imaging of this transgenic strain revealed GFP expression in intestinal cells with a ring pattern consistent with lipid droplet surface localization, revealing hypodermal (epidermal) and intestinal droplets of approximately 1–1.5 μm size (Fig. 4A). In addition, we prepared the nematodes for post-fix Nile red staining, and found that the interior of the ACS-4::GFP rings stains with Nile red, indicating the presence of neutral lipid (Fig. 4B). We
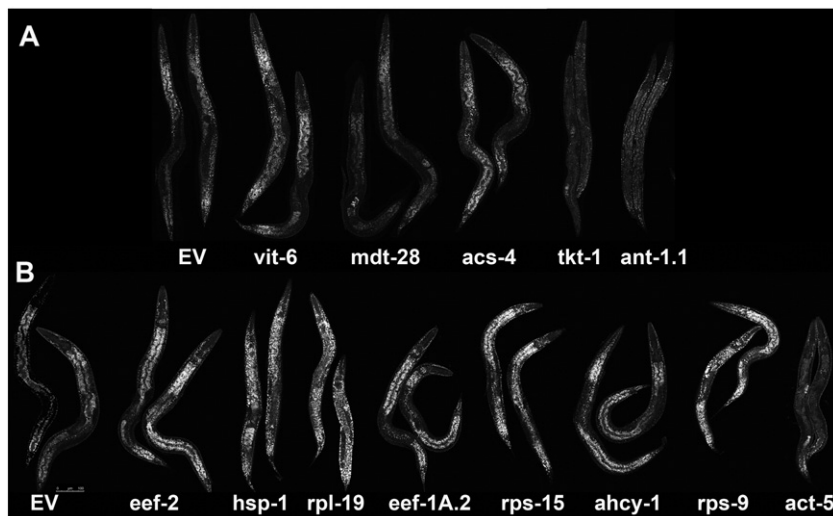

Fig. 2. Post-fix Nile red staining of RNAi knockdown of genes encoding lipid droplet proteins. A. Young adult worms grown on RNAi feeding plates for entire lifetime. Nile red staining shows increased fat accumulation in *vit-6*(*RNAi*) and *acs-4*(*RNAi*) and decreased fat accumulation in *mdt-28*(*RNAi*), *tkt-1*(*RNAi*), and *ant-1.1*(*RNAi*) compared to the empty vector control (EV). B. Young adult worms grown for 24 h on RNAi feeding plates. Increased fat accumulation is apparent after RNAi treatments corresponding to *eef-2*, *hsp-1*, *rpl-19*, *eef-1A.2*, *rps-15*, *ahcy-1*, and *rps-9* compared to empty vector control (EV). Decreased fat accumulation is observed in *act-5*(*RNAi*).
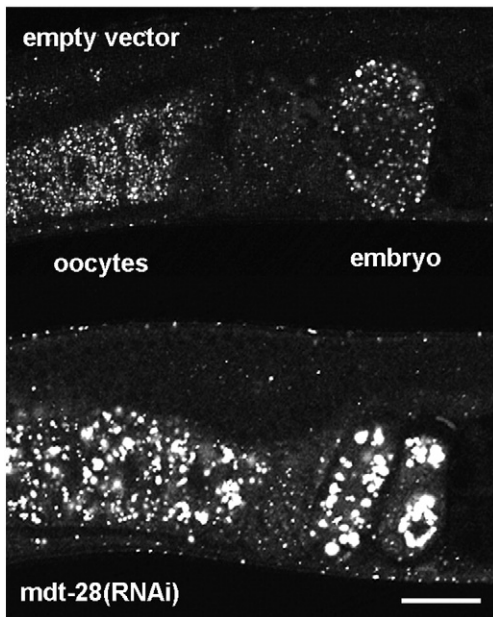
Fig. 3. Knockdown of *mdt-28* leads to clumped lipid droplets in the germ line. Post-fix Nile red staining of empty vector (top worm) and *mdt-28*(*RNAi*) (bottom) visualizing lipid droplets in oocytes and early embryos. The worm uterus contains one embryo that is visible in the empty vector control, while two early embryos are visible in the *mdt-28*(*RNAi*) worm. Size bar is 25 μm.

observed robust ACS-4::GFP expression throughout development in all larval stages and in adult worms. In addition to lipid droplet localization, we observed that ACS-4::GFP is expressed in a range of other tissues, including the pharynx, seam cells, dorsal and ventral nerve cords, and other cells, likely neurons, in the head and tail (Supplemental Fig. 2). Thus, ACS-4 appears to be a resident lipid droplet protein, although it may function in other tissues in *C. elegans* as well.

4. Discussion

Lipid droplets play multiple important roles in cells. In this study, we isolated lipid droplets of the model organism *C. elegans* and report the lipid composition and protein composition of lipid droplets purified from wild type and from high-fat *daf-2* mutant worms. We confirmed that one protein identified in the proteomic analysis, ACS-4, localizes to the surface of *C. elegans* lipid droplets.

As in other organisms, isolated *C. elegans* lipid droplets are composed of a monolayer of the phospholipids PC and PE, surrounding a core of neutral lipids consisting almost exclusively of TAGs. Unlike in mammals, we found that *C. elegans* lipid droplets contain very little cholesterol or cholesterol esters. There are similarities in the lipid composition of *C. elegans* lipid droplets and yolk particles, which are structurally similar to mammalian lipoproteins [48]. In *C. elegans*, both lipid droplets and yolk particles contain mainly PC and PE as major phospholipid species, and both contain TAGs, but very little cholesterol or cholesterol esters. Yolk and lipid droplets differ in that yolk contains large amounts of vitellogenins, which are apoliproteins that contain relatively higher ratios of phospholipids to TAGs [48]. The lipid droplet proteomes of our study and Zhang et al. both showed vitellogenin proteins associated with lipid droplets, which might indicate an association of lipid droplets and yolk particles during yolk biogenesis.

The fatty acid composition of *C. elegans* TAG revealed a high content of dietary fatty acids in lipid droplets. This is consistent with a previous study showing that TAG fractions contained relatively smaller proportions of de novo synthesized fatty acids compared to phospholipid fractions [49]. Similarly, in yeast lipid droplets the cholesterol ester/TAG ratio depends on carbon source [37]. The low amounts of sterols in *C. elegans* lipid droplets is likely a reflection of dietary requirements, in which very low sterol levels are required for growth [49]. It has previously been shown that cholesterol levels are very low in *C. elegans* membranes [38,50], and the main function of cholesterol is for the production of steroid hormones regulating growth and reproduction, rather than as structural components of cellular membranes [51].
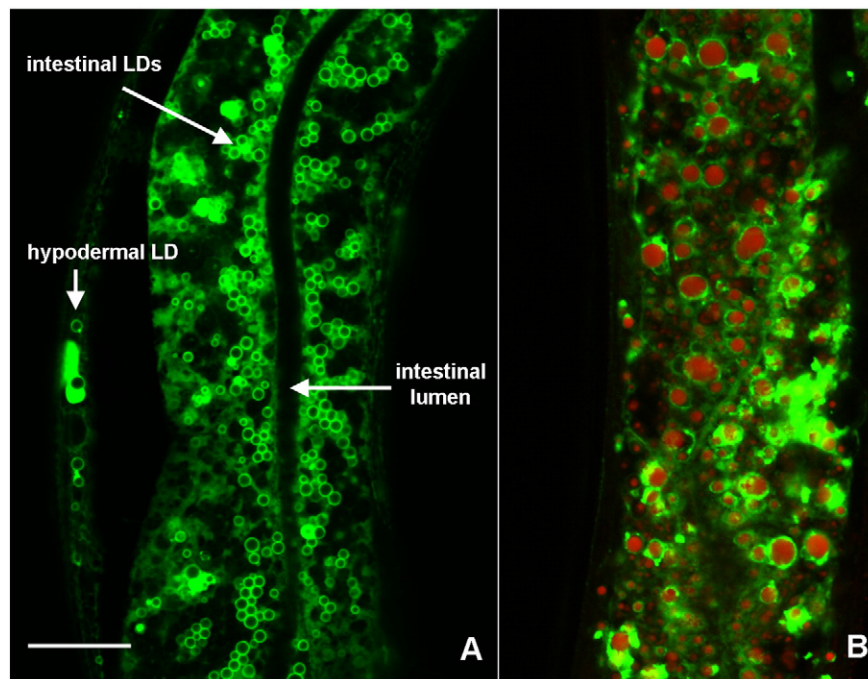

Fig. 4. ACS-4 localizes to hypodermal and intestinal lipid droplets. A. Live imaging of L4 stage ACS-4::GFP strain reveals lipid droplet surface localization throughout the intestine and in the hypodermis. The intestinal lumen is visible in the center of the intestine. B. Post-fix composite image of ACS-4::GFP and Nile red in intestinal tissue. Size bar is 10 μm.

Among the most abundant lipid droplet protein observed in our study and in Zhang et al. [21] was the MDT-28 protein. This protein contains a conserved Perilipin domain in the N terminus, suggesting that MDT-28 is an important structural lipid droplet protein that may play similar structural roles to conserved perilipins. In mammals, perilipins regulate the balance between lipid storage and lipid hydrolysis [10]. The region of homology of MDT-28 to perilipin is in the relatively small region of the protein, identified as a perilipin domain. Interestingly, knockdown of MDT-28 by RNAi had several disparate effects on *C. elegans* lipid droplets. We found that intestinal lipid droplet were somewhat reduced in MDT-28 knockdowns, but lipid droplets in oocytes and embryos appeared to be clustered and showed brighter Nile red staining. MDT-28 has been reported to be expressed in the proximal germ line [52], suggesting an important role for MDT-28 in reproductive tissues.

Many ribosomal proteins were identified in both *C. elegans* proteomes. Ribosomal proteins have been reported in many other lipid droplet proteomes [13,39,40]. The large number of ribosomal proteins identified in the *C. elegans* proteome could be a result of contamination of other cellular compartments. On the other hand, lipid droplets are synthesized on the endoplasmic reticulum, and a population of lipid droplets remains associated with the ER [53]. Furthermore, it is possible that ribosomal subunits could be sequestered in lipid droplets for use later in life, or for packaging into oocytes [54]. The presence of proteins predicted to be associated with mitochondria is also consistent with other reported lipid droplet proteomes, and may suggest a close association of lipid droplets and mitochondria [55,56].

Our proteomic data reached beyond the wild type *C. elegans* strain to examine the long-lived, high-fat *daf-2*(*e1370*) mutants. This strain carries a mutation in the sole insulin-like growth factor receptor in *C. elegans*. Strains carrying this mutation show increased stress resistance and extreme longevity [34,57]. Because the *daf-2* strain contains large lipid droplets and excess fat accumulation, we predicted that different proteins might be associated with lipid droplets in this strain [16]. Therefore, we were surprised to identify very similar proteomes in wild type and *daf-2* mutants, indicating that the lipid droplet proteins are not a major driver of the striking longevity and metabolic differences in *daf-2* mutants.

An important finding of our study was the enrichment of essential proteins as well as proteins that affect fat accumulation in *C. elegans*. Experiments in the fruit fly *Drosophila melanogaster* demonstrate that lipid droplet associated proteins are required to support early development [2]. It is important to note that the fat accumulation defects are not necessarily direct effect of lipid droplets, for example, *act-5*(*RNAi*) worms likely have poor nutrient absorption due to defects in intestinal microvilli [58]. A limitation of our study was that we identified relatively few lipid metabolism proteins. For example, we did not identify DGAT2, which has been shown to associate with *C. elegans* lipid droplets at the ER interface during lipid droplet expansion [20]. Similarly, the atlastin GTPase [17], the lipase ATGL-1 [22], and the CGI-58 homolog coactivator LID-1 [22] did not appear in the proteome of isolated lipid droplets from wild type or *daf-2* mutants. Perhaps these proteins are of relatively low abundance, or alternatively, our purification method may not have allowed for the retention of loosely associated lipid droplet proteins or of proteins that only associate with lipid droplets at the ER interface during lipid droplet expansion.

Our analysis identified new *C. elegans* lipid droplet proteins, including some that affect fat accumulation. One of the few proteins involved in lipid metabolism identified in our proteomic survey was the acyl-CoA synthetase ACS-4. A similar human protein, ACSL3, was shown to be localized to lipid droplets in cultured cells, where it functions to promote lipid droplet biogenesis at the ER [59,60]. Future studies will be necessary to determine whether ACS-4 plays a role in lipid droplet biogenesis or catabolism in *C. elegans*, as well as to confirm the cellular localization and physiological functions of other proteins identified in our proteomic analysis.

Abbreviations

LD	lipid droplet
TAG	triacylglycerol
PC	phosphatidylcholine
PE	phosphtidylethanolamine
TLC	thin layer chromatography
FAMES	fatty acid methyl esters

Supplementary data to this article can be found online at http://dx.doi.org/10.1016/j.bbalip.2015.06.004.

Transparency document

The Transparency document associated with this article can be found, in online version.

Acknowledgements

References

[1] D.J. Murphy, The dynamic roles of intracellular lipid droplets: from archaea to mammals, Protoplasma 249 (2012) 541–585.

[2] Z. Li, M.R. Johnson, Z. Ke, L. Chen, M.A. Welte, Drosophila lipid droplets buffer the H2Av supply to protect early embryonic development, Curr. Biol. 24 (2014) 1485–1491.

[3] Z. Li, K. Thiel, P.J. Thul, M. Beller, R.P. Kuhnlein, M.A. Welte, Lipid droplets control the maternal histone supply of *Drosophila* embryos, Curr. Biol. 22 (2012) 2104–2113.

[4] L.L. Listenberger, X. Han, S.E. Lewis, S. Cases, R.V. Farese Jr., D.S. Ory, J.E. Schaffer, Triglyceride accumulation protects against fatty acid-induced lipotoxicity, Proc. Natl. Acad. Sci. U. S. A. 100 (2003) 3077–3082.

[5] A. Penno, G. Hackenbroich, C. Thiele, Phospholipids and lipid droplets, Biochim. Biophys. Acta (BBA) Mol. Cell Biol. Lipids 1831 (2013) 589–594.

[6] A. Pol, S.P. Gross, R.G. Parton, Biogenesis of the multifunctional lipid droplet: lipids, proteins, and sites, J. Cell Biol. 204 (2014) 635–646.

[7] E. Herker, M. Ott, Unique ties between hepatitis C virus replication and intracellular lipids, Trends Endocrinol. Metab. 22 (2011) 241–248.

[8] N. Krahmer, R.V. Farese, T.C. Walther, Balancing the fat: lipid droplets and human disease, EMBO Mol. Med. 5 (2013) 973–983.

[9] C. Vigouroux, M. Caron-Debarle, C. Le Dour, J. Magre, J. Capeau, Molecular mechanisms of human lipodystrophies: from adipocyte lipid droplet to oxidative stress and lipotoxicity, Int. J. Biochem. Cell Biol. 43 (2011) 862–876.

[10] C. Sztalryd, A.R. Kimmel, Perilipins: lipid droplet coat proteins adapted for tissue-specific energy storage and utilization, and lipid cytoprotection, Biochimie 96 (2014) 96–101.

[11] F. Wilfling, J.T. Haas, T.C. Walther, R.V. Farese Jr., Lipid droplet biogenesis, Curr. Opin. Cell Biol. 29 (2014) 39–45.

[12] C. Thiele, J. Spandl, Cell biology of lipid droplets, Curr. Opin. Cell Biol. 20 (2008) 378–385.

[13] L. Yang, Y. Ding, Y. Chen, S. Zhang, C. Huo, Y. Wang, J. Yu, P. Zhang, H. Na, H. Zhang, Y. Ma, P. Liu, The proteomics of lipid droplets: structure, dynamics, and functions of the organelle conserved from bacteria to humans, J. Lipid Res. 53 (2012) 1245–1253.

[14] C.F. Kurat, H. Wolinski, J. Petschnigg, S. Kaluarachchi, B. Andrews, K. Natter, S.D. Kohlwein, Cdk1/Cdc28-dependent activation of the major triacylglycerol lipase Tgl4 in yeast links lipolysis to cell-cycle progression, Mol. Cell 33 (2009) 53–63.

[15] M. Suzuki, Y. Shinohara, Y. Ohsaki, T. Fujimoto, Lipid droplets: size matters, J. Electron Microsc. 60 (Suppl. 1) (2011) S101–S116.

[16] X. Shi, J. Li, X. Zou, J. Greggain, S.V. Rodkaer, N.J. Faergeman, B. Liang, J.L. Watts, Regulation of lipid droplet size and phospholipid composition by stearoyl-CoA desaturase, J. Lipid Res. 54 (2013) 2504–2514.

[17] R.W. Klemm, J.P. Norton, R.A. Cole, C.S. Li, S.H. Park, M.M. Crane, L. Li, D. Jin, A. Boye-Doe, T.Y. Liu, Y. Shibata, H. Lu, T.A. Rapoport, R.V. Farese Jr., C. Blackstone, H.Y. Guo, H.Y. Mak, A conserved role for atlastin GTPases in regulating lipid droplet size, Cell Rep. 3 (2013) 1465–1475.

[18] A.K. Walker, R.L. Jacobs, J.L. Watts, V. Rottiers, K. Jiang, D.M. Finnegan, T. Shioda, M. Hansen, F. Yang, L.J. Niebergall, D.E. Vance, M. Tzoneva, A.C. Hart, A.M. Naar, A conserved SREBP-1/phosphatidylcholine feedback circuit regulates lipogenesis in metazoans, Cell 147 (2011) 840–852.

[19] S.O. Zhang, A.C. Box, N. Xu, J. Le Men, J. Yu, F. Guo, R. Trimble, H.Y. Mak, Genetic and dietary regulation of lipid droplet expansion in *Caenorhabdtis elegans*, Proc. Natl. Acad. Sci. U. S. A. 107 (2010) 4640–4645.

[20] N. Xu, S.O. Zhang, R.A. Cole, S.A. McKinney, F. Guo, J.T. Haas, S. Bobba, R.V. Farese Jr., H.Y. Mak, The FATP1–DGAT2 complex facilitates lipid droplet expansion at the ER–lipid droplet interface, J. Cell Biol. 198 (2012) 895–911.

[21] P. Zhang, H. Na, Z. Liu, S. Zhang, P. Xue, Y. Chen, J. Pu, G. Peng, X. Huang, F. Yang, Z. Xie, T. Xu, P. Xu, G. Ou, S.O. Zhang, P. Liu, Proteomic study and marker protein identification of *Caenorhabditis elegans* lipid droplets, Mol. Cell. Proteomics 11 (2012) 317–328.

[22] J.H. Lee, J. Kong, J.Y. Jang, J.S. Han, Y. Ji, J. Lee, J.B. Kim, Lipid droplet protein LID-1 mediates ATGL-1-dependent lipolysis during fasting in *Caenorhabditis elegans*, Mol. Cell. Biol. 34 (2014) 4165–4176.

[23] A.G. Fraser, R.S. Kamath, P. Zipperlen, M. Martinez-Campos, M. Sohrmann, J. Ahringer, Functional genomic analysis of *C. elegans* chromosome I by systematic RNA interference, Nature 408 (2000) 325–330.

[24] T. Stiernagle, Maintenance of *C. elegans*, in: T.C.e.R. Community (Ed.), WormBook, 2006 (http://www.wormbook.org).

[25] H. Wang, W.J. Qian, H.M. Mottaz, T.R. Clauss, D.J. Anderson, R.J. Moore, D.G. Camp 2nd, A.H. Khan, D.M. Sforza, M. Pallavicini, D.J. Smith, R.D. Smith, Development and evaluation of a micro- and nanoscale proteomic sample preparation method, J. Proteome Res. 4 (2005) 2397–2403.

[26] G. Depuydt, F. Xie, V.A. Petyuk, N. Shanmugam, A. Smolders, I. Dhondt, H.M. Brewer, D.G. Camp 2nd, R.D. Smith, B.P. Braeckman, Reduced insulin/insulin-like growth factor-1 signaling and dietary restriction inhibit translation but preserve muscle mass in *Caenorhabditis elegans*, Mol. Cell. Proteomics 12 (2013) 3624–3639.

[27] A.M. Mayampurath, N. Jaitly, S.O. Purvine, M.E. Monroe, K.J. Auberry, J.N. Adkins, R.D. Smith, DeconMSn: a software tool for accurate parent ion monoisotopic mass determination for tandem mass spectra, Bioinformatics 24 (2008) 1021–1023.

[28] V.A. Petyuk, A.M. Mayampurath, M.E. Monroe, A.D. Polpitiya, S.O. Purvine, G.A. Anderson, D.G. Camp 2nd, R.D. Smith, DtaRefinery, a software tool for elimination of systematic errors from parent ion mass measurements in tandem mass spectra data sets, Mol. Cell. Proteomics 9 (2010) 486–496.

[29] S. Kim, P.A. Pevzner, MS-GF+ makes progress towards a universal database search tool for proteomics, Nat. Commun. 5 (2014) 5277.

[30] T.J. Brock, J. Browse, J.L. Watts, Genetic regulation of unsaturated fatty acid composition in *C. elegans*, PLoS Genet. 2 (2006) e108.

[31] J.L. Watts, J. Browse, Genetic dissection of polyunsaturated fatty acid synthesis in *Caenorhabditis elegans*, Proc. Natl. Acad. Sci. 99 (2002) 5854–5859.

[32] W.W. Christie, Methods for the separation of the simples classes, in: P.B. Associates (Ed.)Lipid Analysis: Isolation, Separation, Identification and Structural Analysis of Lipids, vol. 15, PJ Barnes & Associates, Bridgwater, England 2003, p. 110.

[33] E.C. Pino, C.M. Webster, C.E. Carr, A.A. Soukas, Biochemical and High Throughput Microscopic Assessment of Fat Mass in *Caenorhabditis elegans*, 2013. e50180.

[34] C. Kenyon, J. Chang, E. Gensch, A. Rudner, R. Tabtiang, A *C. elegans* mutant that lives twice as long as wild type, Nature 366 (1993) 461–464.

[35] K. Tauchi-Sato, S. Ozeki, T. Houjou, R. Taguchi, T. Fujimoto, The surface of lipid droplets is a phospholipid monolayer with a unique fatty acid composition, J. Biol. Chem. 277 (2002) 44507–44512.

[36] R. Bartz, W.H. Li, B. Venables, J.K. Zehmer, M.R. Roth, R. Welti, R.G. Anderson, P. Liu, K.D. Chapman, Lipidomics reveals that adiposomes store ether lipids and mediate phospholipid traffic, J. Lipid Res. 48 (2007) 837–847.

[37] K. Grillitsch, M. Connerth, H. Kofeler, T.N. Arrey, B. Rietschel, B. Wagner, M. Karas, G. Daum, Lipid particles/droplets of the yeast *Saccharomyces cerevisiae* revisited: lipidome meets proteome, Biochim. Biophys. Acta 1811 (2011) 1165–1176.

[38] M. Merris, W.G. Wadsworth, U. Khamrai, R. Bittman, D.J. Chitwood, J. Lenard, Sterol effects and sites of sterol accumulation in *Caenorhabditis elegans*: developmental requirement for 4alpha-methyl sterols, J. Lipid Res. 44 (2003) 172–181.

[39] M. Beller, D. Riedel, L. Jv§nsch, G. Dieterich, J.r. Wehland, H. Jv§ckle, R.P. Kv°hnlein, Characterization of the *Drosophila* lipid droplet subproteome, Mol. Cell. Proteomics 5 (2006) 1082–1094.

[40] S. Cermelli, Y. Guo, S.P. Gross, M.A. Welte, The lipid-droplet proteome reveals that droplets are a protein-storage depot, Curr. Biol. 16 (2006) 1783–1795.

[41] Y. Ding, S. Zhang, L. Yang, H. Na, P. Zhang, H. Zhang, Y. Wang, Y. Chen, J. Yu, C. Huo, S. Xu, M. Garaiova, Y. Cong, P. Liu, Isolating lipid droplets from multiple species, Nat. Protoc. 8 (2013) 43–51.

[42] N. Krahmer, M. Hilger, N. Kory, F. Wilfling, G. Stoehr, M. Mann, R.V. Farese Jr., T.C. Walther, Protein correlation profiles identify lipid droplet proteins with high confidence, Mol. Cell. Proteomics 12 (2013) 1115–1126.

[43] J.S. Tan, C.J. Seow, V.J. Goh, D.L. Silver, Recent advances in understanding proteins involved in lipid droplet formation, growth and fusion, J. Genet. Genomics 41 (2014) 251–259.

[44] P. Lu, C. Vogel, R. Wang, X. Yao, E.M. Marcotte, Absolute protein expression profiling estimates the relative contributions of transcriptional and translational regulation, Nat. Biotechnol. 25 (2007) 117–124.

[45] R.S. Kamath, A.G. Fraser, Y. Dong, G. Poulin, R. Durbin, M. Gotta, A. Kanapin, N. Le Bot, S. Moreno, M. Sohrmann, D.P. Welchman, P. Zipperlen, J. Ahringer, Systematic functional analysis of the *Caenorhabditis elegans* genome using RNAi, Nature 421 (2003) 231–237.

[46] Z. Liu, X. Li, Q. Ge, M. Ding, X. Huang, A lipid droplet-associated GFP reporter-based screen identifies new fat storage regulators in *C. elegans*, J. Genet. Genomics 41 (2014) 305–313.

[47] R.A. Coleman, T.M. Lewin, C.G. Van Horn, M.R. Gonzalez-Baro, Do long-chain acyl-CoA synthetases regulate fatty acid entry into synthetic versus degradative pathways? J. Nutr. 132 (2002) 2123–2126.

[48] H.M. Kubagawa, J.L. Watts, C. Corrigan, J.W. Edmonds, E. Sztul, J. Browse, M.A. Miller, Oocyte signals derived from polyunsaturated fatty acids control sperm recruitment in vivo, Nat. Cell Biol. 8 (2006) 1143–1148.

[49] C.L. Perez, M.R. Van Gilst, A ^{13}C isotope labeling strategy reveals the influence of insulin signaling on lipogenesis in *C. elegans*, Cell Metab. 8 (2008) 266–274.

[50] T.V. Kurzchalia, S. Ward, Why do worms need cholesterol? Nat. Cell Biol. 5 (2003) 684–688.

[51] N. Fielenbach, A. Antebi, *C. elegans* dauer formation and the molecular basis of plasticity, Genes Dev. 22 (2008) 2149–2165.

[52] W. Chi, V. Reinke, Promotion of oogenesis and embryogenesis in the *C. elegans* gonad by EFL-1/DPL-1 (E2F) does not require LIN-35 (pRB), Development 133 (2006) 3147–3157.

[53] J.K. Zehmer, R. Bartz, B. Bisel, P. Liu, J. Seemann, R.G. Anderson, Targeting sequences of UBXD8 and AAM-B reveal that the ER has a direct role in the emergence and regression of lipid droplets, J. Cell Sci. 122 (2009) 3694–3702.

[54] M.A. Welte, Proteins under new management: lipid droplets deliver, Trends Cell Biol. 17 (2007) 363–369.

[55] S. Larsson, S. Resjo, M.F. Gomez, P. James, C. Holm, Characterization of the lipid droplet proteome of a clonal insulin-producing beta-cell line (INS-1 832/13), J. Proteome Res. 11 (2012) 1264–1273.

[56] H. Zhang, Y. Wang, J. Li, J. Yu, J. Pu, L. Li, H. Zhang, S. Zhang, G. Peng, F. Yang, P. Liu, Proteome of skeletal muscle lipid droplet reveals association with mitochondria and apolipoprotein a-I, J. Proteome Res. 10 (2011) 4757–4768.

[57] C.T. Murphy, P. Hu, Insulin/insulin-like growth factor signaling in *C. elegans*, in: T.C.e.r. community (Ed.), Wormbook, 2013.

[58] F. Farina, A. Alberti, N. Breuil, M. Bolotin-Fukuhara, M. Pinto, E. Culetto, Differential expression pattern of the four mitochondrial adenine nucleotide transporter ant genes and their roles during the development of *Caenorhabditis elegans*, Dev. Dyn. 237 (2008) 1668–1681.

[59] M. Poppelreuther, B. Rudolph, C. Du, R. Grossmann, M. Becker, C. Thiele, R. Ehehalt, J. Fullekrug, The N-terminal region of acyl-CoA synthetase 3 is essential for both the localization on lipid droplets and the function in fatty acid uptake, J. Lipid Res. 53 (2012) 888–900.

[60] A. Kassan, A. Herms, A. Fernandez-Vidal, M. Bosch, N.L. Schieber, B.J. Reddy, A. Fajardo, M. Gelabert-Baldrich, F. Tebar, C. Enrich, S.P. Gross, R.G. Parton, A. Pol, Acyl-CoA synthetase 3 promotes lipid droplet biogenesis in ER microdomains, J. Cell Biol. 203 (2013) 985–1001.